

# Biogenic Synthesis of Photocatalytically Active Nickel Oxide (NiO) Nanoparticles using *Catharanthus roseus* Leaf Extract

K.Usha<sup>1</sup>, K.Karthik<sup>2</sup>, T.Kavitha<sup>1\*</sup>, Keerthi<sup>2</sup>

<sup>1</sup> Department of Physics, Shrimathi Devkunvar Nanalal Bhatt Vaishnav College for Women (Autonomous), Chromepet, Chennai–600044.

<sup>2</sup> Department of Chemistry, College of Engineering Guindy (CEG), Anna University, Chennai–600025.

\*Corresponding author's E-mail: [kavithatphd@gmail.com](mailto:kavithatphd@gmail.com)

## Abstract

A simple and environmentally friendly method was employed to synthesize Nickel oxide (NiO) nanoparticles (NPs) using the leaf extract of *Catharanthus roseus* via the sol-gel method. Nickel sulfate hexahydrate was utilized as a precursor, with the leaf extract of *Catharanthus roseus* serving as both a reducing agent and a stabilizing agent. Various characterization techniques including X-ray diffraction, Fourier transfer infrared spectroscopy, Ultraviolet diffused reflectance spectroscopy (UV-DRS), Scanning electron microscopy, Energy dispersive X-ray analysis, Transmission electron microscopy, and Vibrating sample magnetometer were employed to investigate the structural and characteristic properties of the NiO NPs. The synthesized NiO NPs showed super paramagnetic behaviour at room temperature with saturated magnetization ( $M_s = 47.22 \times 10^{-3}$  emu). Methylene blue is one of the industrial dyes that make water unfit for irrigation or drinking. It is a toxic, carcinogenic and recalcitrant dye which causes a severe threat to human health. As the dye is difficult to be degraded, a biological eco-friendly method is followed in the present study. NiO NPs had a band energy gap of 3.6 eV and a strong potential to be used as photocatalysts in wastewater treatment to rapidly degrade textile dyes. Almost complete photocatalytic degradation of methylene blue dye was achieved using NiO NPs, which also exhibited high stability and reusability for three additional cycles without any significant decrease in efficacy.

**Keywords:** Biogenic synthesis; *Catharanthus roseus*; Nickel oxide nanoparticles; Photocatalysts; Methylene Blue; Water treatment

## Introduction

The rapid growth of industrialization of the country has increased the release of large amounts of dyes and heavy metals through their runoff into the water bodies thus contaminating a number of water bodies [1]. Increasing environmental pollution has led scientists worldwide to develop photocatalysts for the purification of water contaminated with various pollutants [2]. Photocatalytic degradation of organic pollutants represents a promising technology for water treatment, offering a simple and efficient method that generates non-toxic end products. [3]. Nano science and nanotechnology have recently experienced remarkable growth due to their numerous applications in various domains. Metal oxide (MO) based nanoparticles have been widely used in electrochemical films, smart windows and photocatalysis. MOs such as ZnO, CeO<sub>2</sub>, TiO<sub>2</sub>, SnO<sub>2</sub>, CuO, WO<sub>3</sub> and

NiO have been widely used as photocatalysts towards the abatement of organic dyes and contaminants from wastewater [2,4]. The NiO NPs are of interest in recent years due to their superior catalytic activity with unique properties like high electron mobility and chemical stability [5]. Recently, NiO NPs have been employed in wastewater treatment technologies and sensor applications [6].

NiO is a p-type semiconductor widely used as an effective absorbent and visible light photocatalyst due to its high super lattice in the inbound orbital and conduction regions [7]. Various methods have been utilized to synthesize tunable NiO NPs with desired band gaps and morphologies. The size and morphology depends on the synthetic techniques such as high energy ball milling, sol-gel, co-precipitation, micro-emulsion, hydrothermal, microwave, sono-chemical, chemical vapour deposition and pulsed laser ablation [8]. The sol-gel method stands out to be the best over the other methods as it offers a range of benefits such as low temperature synthesis with pure products [9]. In recent years, researchers have focused on synthesizing NPs using plant extracts, thus opening a new era towards non-toxic synthetic methods. The biogenic method of synthesis is cost-effective and non-toxic. When using plant extracts as reducing and capping agents, the synthesis of nanoparticles (NPs) can be efficiently achieved with minimal environmental impact. This method leverages natural plant compounds to facilitate the formation and stabilization of NPs, making it an attractive alternative to conventional chemical synthesis methods. Researchers have reported that the plant extracts have the potential of shaping up of the NPs. Shape of the NPs directly influences the particle size distribution which in turn has an effect on the band gap [10–12].

*Catharanthus roseus*, a vital medicinal plant, is a member of the Apocynaceae family widely used in traditional herbal medicine and its secondary metabolites have been used to treat cancer. The major phytochemicals of its leaf extract are flavonoids, saponins and alkaloids. Many parts of this plant have been used for therapeutic purposes such as diabetes, Alzheimer's disease and cancer [13]. The plant produces two major terpene indole alkaloids (vincristine and vinblastine) that fight cancer [14]. Studies have demonstrated that the leaf juice of *Catharanthus roseus* can lower blood glucose levels in both normal and alloxan-induced diabetic rabbits [15]. Furthermore, the leaf extract serves as a natural reducing agent in the sol-gel method for synthesizing NiO NPs.

In this study, the leaf extract was used to reduce nickel salt to NiO nanoparticles using the sol-gel method. The synthesized nanoparticles were characterized using XRD, FT-IR, SEM-EDS, TEM, UV-DRS, and VSM. Additionally, the photocatalytic activity of the synthesized NiO NPs was employed to degrade methylene blue (MB), a common pollutant found in textile industry effluents.

## Methodology

### 2.1 Preparation of leaf extracts of *Catharanthus roseus*

A quantity of 50g of cut leaves of *Catharanthus roseus* was refluxed at 70-80°C for 2 hours with deionized water in round bottom flask. The resulting golden yellow colour extract was further filtered and used as a reducing agent in the sol-gel method for synthesizing NiO NPs.

### 2.2 Synthesis of Nickel Oxide Nanoparticles using *Catharanthus roseus* Leaf Extract

Nickel oxide nanoparticles were synthesized using leaf extract of *Catharanthus roseus* and nickel sulphate hexahydrate (precursor) via sol-gel method (Fig.1). Twenty millimolar solution of nickel sulphate hexahydrate was prepared using deionized water. The leaf extract was added drop wise to the nickel precursor solution with vigorous stirring. After stirring for 2-3 hours, 0.5 M sodium hydroxide (NaOH) was added slowly till a green colour precipitate formed. Alkaline pH was maintained for complete precipitation of nickel ions. The precipitate was stirred for 24 hours and washed several times using deionized water. Before calcination, the

precipitate as dried in a hot air oven at 80°C for 2 hours and finely powdered. In muffle furnace, the powder was calcinated at 450°C for 2 hours, pulverized and stored for further analysis.

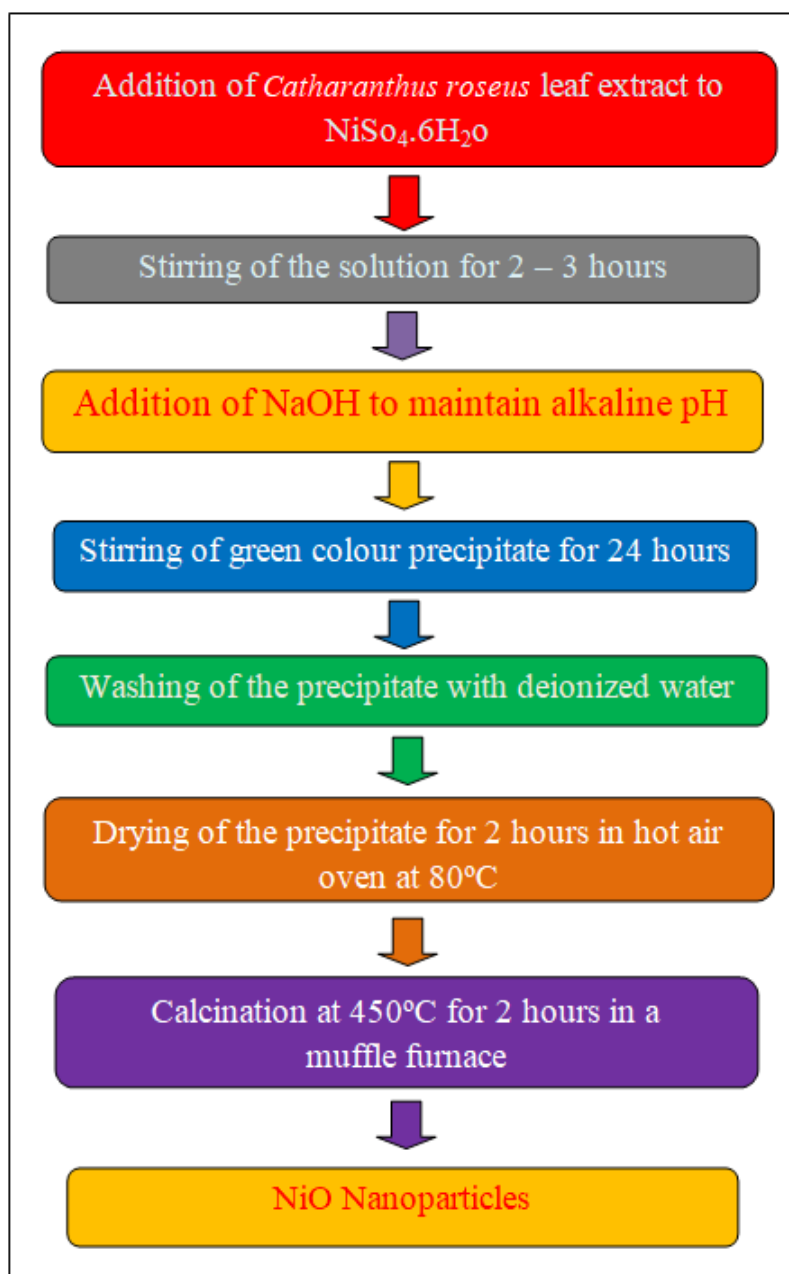


**Fig.1.** Preparation of NiO NPs using Sol-Gel method

### 2.3 Characterization of Nickel Oxide Nanoparticles

The shape and optical characteristics of the synthesized green NiO NPs were confirmed by powder XRD using Cu K $\alpha$  radiation ( $\lambda = 0.1544$  nm) at Smart Lab SE X-Ray, Rigaku Japan. The functional group analysis was done using Shimadzu IRAffinity-1FT-IR Spectrophotometer in potassium bromide (KBr) pellet mode. The synthesized NiO NPs optical band gap was characterized by UV-visible Spectrophotometer in Diffused Reflectance Spectrum (DRS) using Jasco V650 with ISV722 between 200 to 800 nm. The morphological and elemental analysis was carried out by SEM with an EDX analyzer using TESCAN VEGA3 SBH operating at 30kV using tungsten filaments as an electron source. The surface morphology was studied using FEITecni G<sup>2</sup> 20 S-TWIN TEM operating at 200 kV with a LaB<sub>6</sub>/W emitter as an electron source. The

magnetic property was studied using Lakeshore VSM 7410 Vibrating Sample Magnetometer (VSM) at room temperature.

## 2.4. Photocatalytic Activity of Nickel Oxide Nanoparticles

Photocatalytic activity is an effective method for dye degradation. The dye used for this study is methylene blue. Methylene blue is an organic dye of the Phenothiazine family that is vibrant greenish blue in color. A solution of 5ppm of methylene blue ( $C_{16}H_{18}ClN_3S$ ) was prepared in deionized water. AUV-vis spectrophotometer (Jasco V730) was used to measure the absorbance of the MB solutions. For photocatalytic activity, optimization parameters such as concentration of catalyst, concentration of dye were recorded with different time intervals. The synthesized photocatalyst was suspended in 50mL of MB dye solution under constant stirring using a magnetic stirrer. The MB dye solution was then placed in dark for 30 minutes to attain adsorption-desorption equilibrium. The solution was kept in both natural sunlight and visible light photoreactors for the degradation of MB. The absorbance was regularly monitored at every 15 minutes using the UV-visible spectrophotometer to check the degradation of MB dye. Optimization studies were carried out to fix the ideal dose of catalyst, concentration of dye and time for photocatalytic degradation of MB.

## 3. Results and Discussion

### 3.1 Structural and Phase Analysis by XRD

The powder XRD was used for phase identification of the synthesized NiO nanoparticles (NiO NPs) as shown in the XRD diffractogram (Fig. 2). The peaks were indexed using JCPDS Card No. 47-1049, with an intense peak at  $43.36^\circ$  corresponding to the (200) plane of NiO, indicating the formation of a face-centered cubic (FCC) crystal structure with lattice parameter  $a = 4.0 \text{ \AA}$ . Similar to our studies, Mamta Bulla *et al.* [16] have reported the same findings. The researcher have reported the other two peaks, which are located at an angle  $2\theta$  of  $30.92^\circ$  (Abishak kumar *et al*) and  $51.6^\circ$  (Shabbir Hussain *et al*) were determined to be  $Ni_2O_3$  [17,18]. The crystallite size (D) was determined using the Debye-Scherrer formula (equation 1) and was found to be 12.93 nm, where K is a constant (0.94),  $\lambda$  is the wavelength of Cu  $K\alpha$  radiation ( $1.54 \text{ \AA}$ ),  $\beta$  is the FWHM, and  $\theta$  is the diffraction angle.

$$D = K\lambda / \beta \cos(\theta) \quad (1)$$

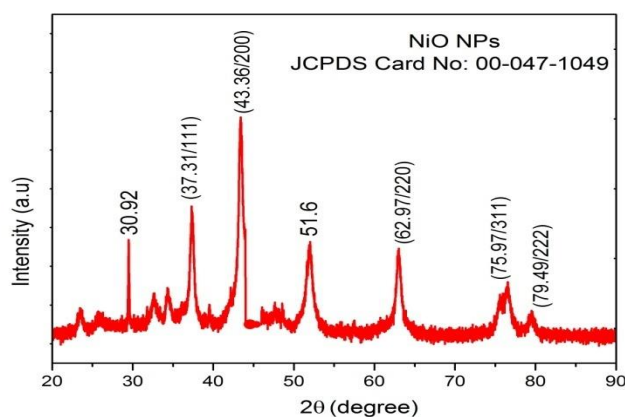


Fig.2.XRD diffractogram of synthesized NiO NPs

### 3.2 Functional Group Analysis and Confirmation by FT-IR

The characteristic peaks in the range of 400-4000  $\text{cm}^{-1}$  in the FT-IR spectrum confirmed the presence of functional groups. The FT-IR spectrum (Fig. 3) showed minor peaks at 1041 and 1116  $\text{cm}^{-1}$ , confirming the presence of trace amounts of polyphenol groups from the plant extract [17]. The characteristic vibration peak at 545  $\text{cm}^{-1}$  corresponds to the stretching frequencies of the metal-oxygen bond (Ni-O), which is usually observed between 400 and 700  $\text{cm}^{-1}$  [18]. The peak observed at 1630  $\text{cm}^{-1}$  is attributed to the bending mode of water present in the lattice of the NiO NPs [19]. The peak at 1381  $\text{cm}^{-1}$  is attributed to the bending modes of the C-H bond, while the peak at 2900  $\text{cm}^{-1}$  is due to the asymmetric stretching of C-H in  $\text{CH}_2$  groups of the plant extract [19, 20]. Additionally, A. A. Olajire *et al.* [21] reported a peak at 3400  $\text{cm}^{-1}$  due to the N-H stretching mode of the plant extract bound to the NiO NPs as capping and stabilizing agents.

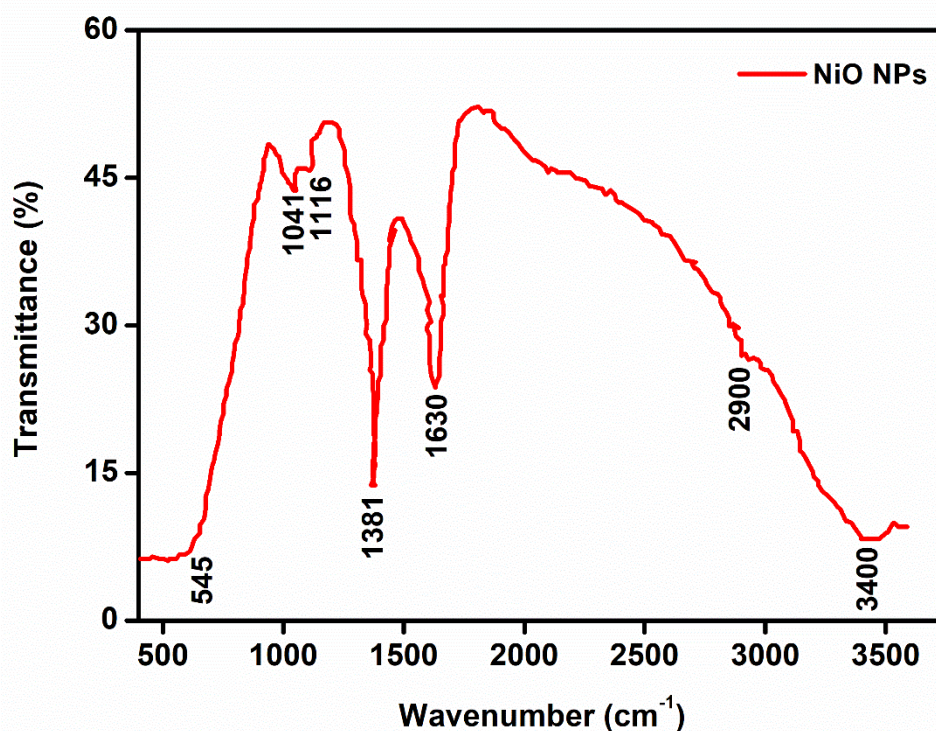
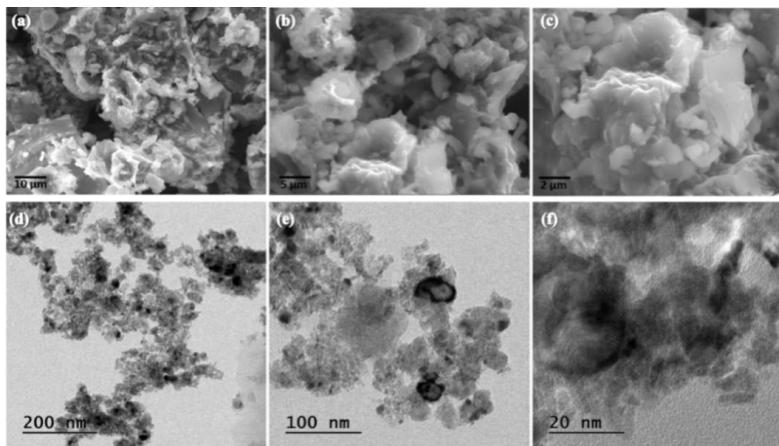


Fig.3. FT-IR spectrum of green synthesized NiO NPs

### 3.3 Morphological and Elemental Analysis

The green synthesized NiO nanoparticles showed agglomerated irregular hexagonal shaped particles [5,22]. The sizes of the nanoparticles ranged from 50 to 100 nm in random orientation with irregular surfaces. The HR-TEM clearly indicated the lattice fringes and d-spacing seen in the NiO nanoparticles. The SEM micrographs showed large agglomerated irregular and randomly oriented hexagonal plate-like structures. The large agglomerated particles self assembled to form plate-like structures (Fig.4). According to the elemental mapping, the EDX examination only detects the presence of nickel and oxygen (Fig.5). The compositional analysis reveals the presence of Nickel (Ni) and Oxygen (O) in the plate-like structures (Table 1).



**Fig.4.**(a, b,c) SEM micrographs, (d,e) TEM micrographs in various magnifications and (f) HR-TEM micrograph of green synthesized NiO NPs

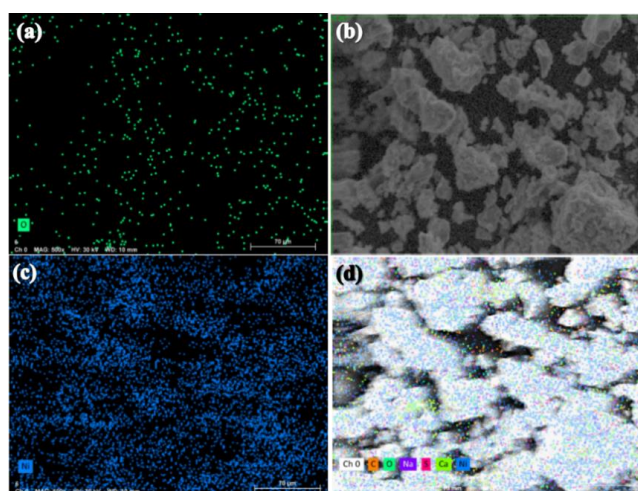


**Fig. 5.**Elemental mapping of (a) oxygen, (c) nickel of green synthesized NiO NPs

Element	Composition (%)
Nickel (Ni)	76.21
Oxygen (O)	23.79

**Table 1.**Elemental composition using EDX analysis of green synthesized NiO NPs

### 3.4Optical Studies using UV-DRS

The UV-DRS spectra were recorded in the range of 200-800 nm to find the absorption region and the band gap energy of the photocatalyst. Maximum absorption was observed at 340 nm in the green synthesized NiO nanoparticles (Fig.6a). According to Tauc plot (Fig.6b), the diffusive reflectance mode in the UV-visible region had an optical band gap of 3.6 eV, which is similar to the results obtained have reported a band gap of 3.55 eV [23]. The formula in equation (2) is used to determine the optical band gap energy of the synthesized NiO photocatalysts.

$$E_g = 1240/\lambda_{\text{edge}} \quad (2)$$

where  $E_g$  is the optical band gap energy and 1240 is the constant derived from the relationship between frequency and wavelength as shown in equation(3) [24].

$$E = hc/\lambda \quad (3)$$

Where  $\lambda$  (nm) is the wavelength,  $c$  is the speed of light in the vacuum ( $3 \times 10^8 \text{ ms}^{-1}$ ) and  $h$  is Planck's constant ( $6.62607015 \times 10^{-34} \text{ Js}$ ).

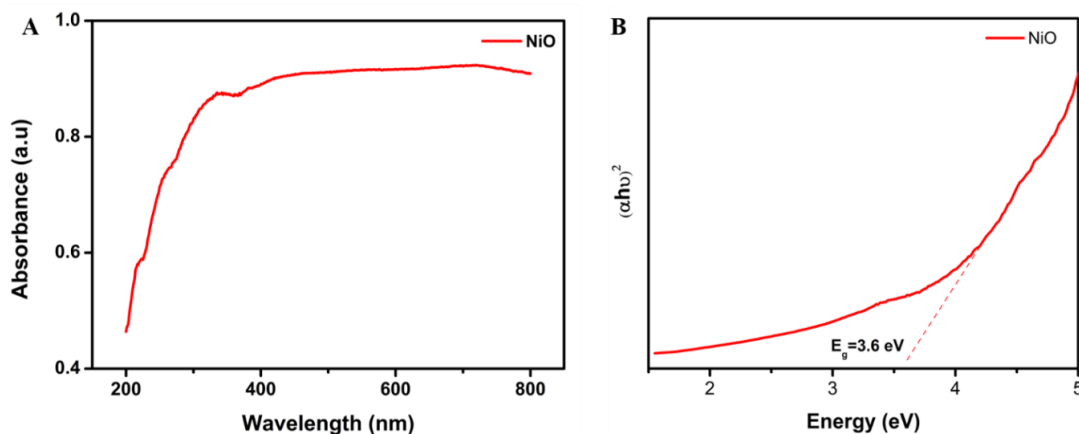


**Fig.6.** (a) UV-DRS Spectra and (b) Tauc Plot of green synthesized NiO NPs

### 3.5 Magnetic Studies using VSM

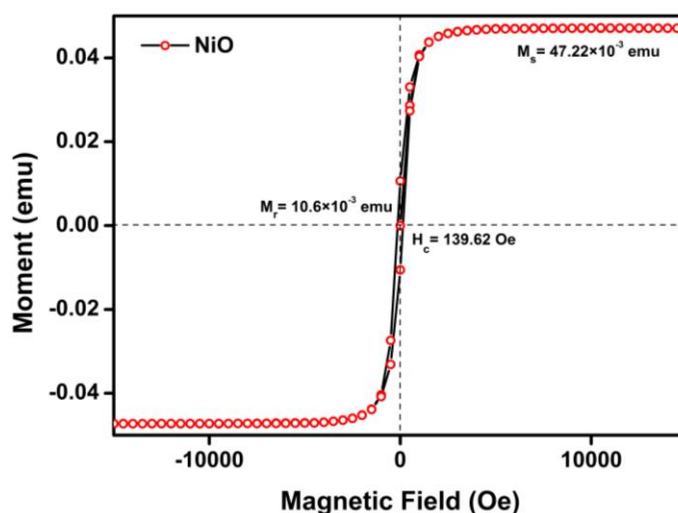


**Fig.7.** Magnetic hysteresis ( $M-H$ ) curve measurement for green synthesized NiO NPs

VSM is a scientific tool that uses Faraday's law of induction to detect magnetic properties. The Magnetization-Field ( $M-H$ ) hysteresis loop for the green synthesized NiO NPs was carried out at room temperature (Fig.7)[25]. The hysteresis curve of nickel oxide nanoparticles showed various properties such as saturated magnetization ( $M_s = 47.22 \times 10^{-3} \text{ emu}$ ), retentively ( $M_r = 10.6 \times 10^{-3} \text{ emu}$ ) and coercive field ( $H_c = 139.62 \text{ Oe}$ ). Magnetization is improved by decreasing the particle size, that leads to increased surface atoms and uncompensated surface spins, resulting in greater magnetization [26]. According to the VSM, the saturated magnetization value  $47.22 \times 10^{-3} \text{ emu}$  is observed in the NiO NPs, which displays super paramagnetic behavior [27]. Super paramagnetism

happens in nanoparticles that possess a single domain and this is attainable when the diameter of the particles is less than 50 nm [28]. The magnetization of NiO NPs increased because of the lack of change in saturation when the magnetic strength was increased to 10k Oe. The existence of the super magnetic particles can be attributed to the electrical arrangement of uncompensated spins on the surface level [29]. Therefore, the observed super magnetic behavior of the green synthesized NiO NPs can be attributed to the reduction in size as supported by the XRD results.

### 3.6 Photocatalytic Activity of NiO NPs

Experiments were conducted to optimize parameters such as the amount of catalyst required and the concentration of the dye [30]. As shown in Fig. 9 (a, b), the optimized conditions for the photocatalytic degradation of MB are 40 mg of catalyst in a 5 ppm (50 ml) dye solution under visible light irradiation for 90 minutes. Fig. 8 shows the degradation of methylene blue by NiO NPs for the time interval (90 mins). The photocatalytic studies were performed in a photoreactor and in natural sunlight. The NiO photocatalyst showed greater efficiency of 98% in the photoreactor compared to 45% in natural sunlight. In concordance with the present study, Alzaqri *et al* [31] achieved a maximum of 97% methylene blue degradation.

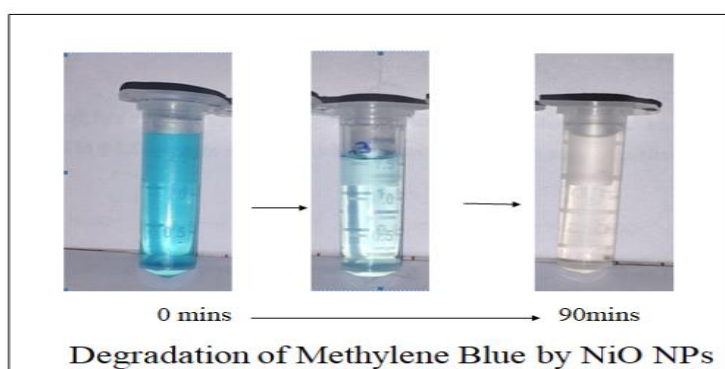


**Fig.8.** Degradation of Methylene Blue by NiO NPs

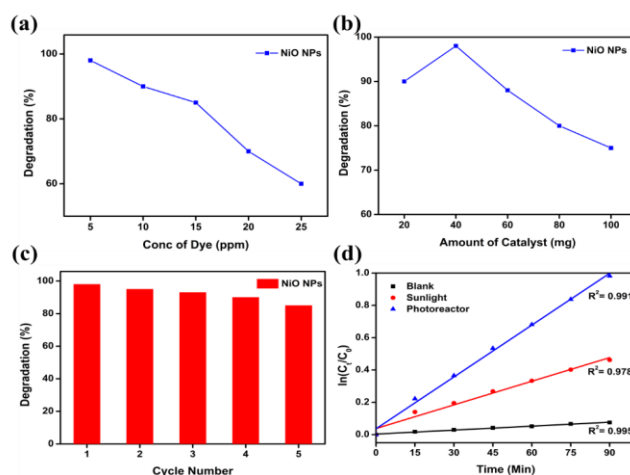


**Fig.9.**Effect of (a) concentration of dye, (b) amount of catalyst, (c) reusability and kinetic studies of NiO NPs.

The study revealed that the light source from the photo reactor is efficient in producing the active/radical species for the photo degradation of MB dye compared to natural sunlight, which is a combination of UV and visible light with less intensity [32]. During the advanced oxidation processes (AOPs) the photo generated electrons

and holes combine with oxygen and hydronium ions generating free radical hydroxyls ( $\bullet\text{OH}$ ) which are active species responsible for the photo degradation of MB dye [33]. Equation (4-6) provides the potential process for the degradation of methylene blue dye using synthesized NiO NPs.

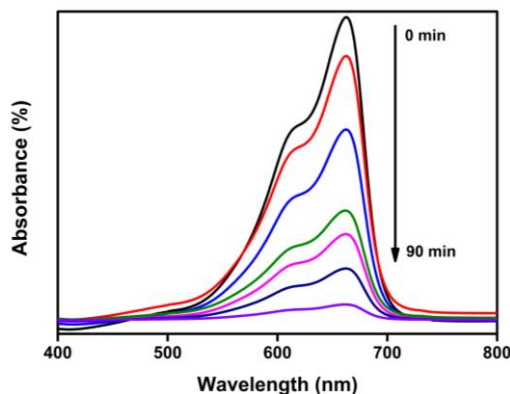
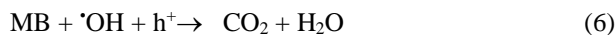


**Fig.10.** Photodegradation of MB using green synthesized NiO NPs under optimized conditions

The photocatalysis of MB by the green synthesized NiO NPs under optimized conditions is shown in Fig.10 over a period of time. The photo degradation of MB dye using NiO NPs follows first-order reaction kinetics as shown in Fig.9(d) [34]. All the fitted curves are shown in Fig.9 (d) plotted between time (t) vs.  $\ln(C_t/C_0)$  exhibited a linear fashion with the regression coefficient ( $R^2$ ) of 0.97-0.99. The rate constant of NiO NPs in photoreactor was higher compared to natural sunlight. This infers that photoreactor provides an optimal light source for best photocatalytic activity. Reusability study was carried out with optimized conditions against MB. The synthesized NiO NPs demonstrated good reusability for up to three cycles, retaining more than 93% of their initial activity (Fig.9(c)). A gradual decrease in efficiency was observed in the fourth cycle due to the deactivation of the catalyst's active sites [35].

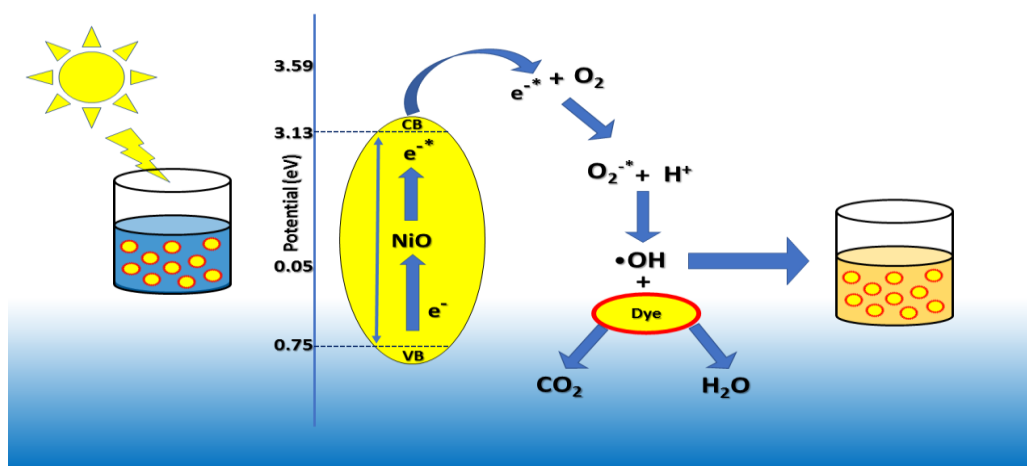


**Fig.11.** Schematic representation of the mechanism for photocatalytic activity

#### 4. Conclusion

*Catharanthus roseus* leaf extract was utilized for synthesizing nickel oxide nanoparticles via the biogenic sol-gel method. The formation of face-centered cubic and hexagonal-shaped NiO NPs, along with an energy band gap of 3.6 eV, was confirmed by XRD, HR-TEM, and UV-DRS analyses. The green-synthesized NiO NPs exhibited remarkable super paramagnetic properties. They demonstrated excellent photocatalytic activity, achieving 98% degradation of MB dye under visible light compared to natural sunlight. Optimization studies indicated that 40 mg of NiO NPs catalyst decolorizes MB dye in 90 minutes. The degradation reaction followed a first-order kinetics with a high regression coefficient ( $R^2 = 0.99$ ). Overall, this study underscores the remarkable photocatalytic activity of synthesized NiO NPs in wastewater treatment, highlighting their eco-friendly and non-toxic nature, high stability, and reusability as effective absorbents.

#### Declaration of Competing Interest

The authors declare that they have no know competing interests or personal relationships that could have appeared to influence the work reported in this paper.

#### Acknowledgment

Authors are grateful to Dr. A. Rajeswari and Dr. P. Koteeswari, SDNB Vaishnav College for Women, Dr. R. Selvarajan, Centre for Nano Science and Technology, Anna University and Mr. V. Ragavendran, Madurai Kamaraj University for all the characterization facilities and support.

#### References

- [1] P. Koteeswari, S. Sagadevan, I. Fatimah, A. Kassegn Sibhatu, S. Izwan Abd Razak, E. Leonard, T. Soga, Green synthesis and characterization of copper oxide nanoparticles and their photocatalytic activity, *Inorg. Chem. Commun.* 144 (2022) 109851. <https://doi.org/10.1016/j.inoche.2022.109851>.
- [2] A. Angel Ezhilarasi, J. Judith Vijaya, K. Kaviyarasu, L. John Kennedy, R.J. Ramalingam, H.A. Al-Lohedan, Green synthesis of NiO nanoparticles using *Aegle marmelos* leaf extract for the evaluation of in-vitro cytotoxicity, antibacterial and photocatalytic properties, *J. Photochem. Photobiol. B Biol.* 180 (2018) 39–50. <https://doi.org/10.1016/J.JPHOTOBIOB.2018.01.023>.
- [3] T. Lv, L. Pan, X. Liu, T. Lu, G. Zhu, Z. Sun, Enhanced photocatalytic degradation of methylene blue by ZnO-reduced graphene oxide composite synthesized via microwave-assisted reaction, *J. Alloys Compd.* 509 (2011) 10086–10091. <https://doi.org/10.1016/J.JALLCOM.2011.08.045>.
- [4] F.U. Rehman, R. Mahmood, M. Ben Ali, A. Hedfi, A. Mezni, S. Haq, S.U. Din, R. Ehsan, Physicochemical, Photocatalytic, Antibacterial, and Antioxidant Screening of *Bergenia Ciliata* Mediated Nickel Oxide Nanoparticles, *Crystals*. 11 (2021) 1137. <https://doi.org/10.3390/cryst11091137>.
- [5] F.T. Thema, E. Manikandan, A. Gurib-Fakim, M. Maaza, Single phase Bunsenite NiO nanoparticles green synthesis by *Agathosma betulina* natural extract, *J. Alloys Compd.* 657 (2016) 655–661. <https://doi.org/10.1016/J.JALLCOM.2015.09.227>.
- [6] F.A. Harraz, R.M. Mohamed, A. Shawky, I.A. Ibrahim, Composition and phase control of Ni/NiO nanoparticles for photocatalytic degradation of EDTA, *J. Alloys Compd.* 508 (2010) 133–140. <https://doi.org/10.1016/J.JALLCOM.2010.08.027>.
- [7] S. Pooyandeh, S. Shahidi, A. Khajehnezhad, R. Mongkholrattanasit, In situ deposition of NiO nanoparticles on cotton fabric using sol–gel method- photocatalytic activation properties, *J. Mater. Res. Technol.* 12 (2021) 1–14. <https://doi.org/10.1016/J.JMRT.2021.02.056>.
- [8] M. Ghosh, K. Biswas, A. Sundaresan, C.N.R. Rao, MnO and NiO nanoparticles: synthesis and magnetic properties, *J. Mater. Chem.* 16 (2006) 106–111. <https://doi.org/10.1039/B511920K>.
- [9] Z. Sabouri, A. Akbari, H.A. Hosseini, M. Khatami, M. Darroudi, Green-based bio-synthesis of nickel oxide nanoparticles in Arabic gum and examination of their cytotoxicity, photocatalytic and antibacterial effects, *Green Chem. Lett. Rev.* 14 (2021) 404–414.

- <https://doi.org/10.1080/17518253.2021.1923824>.
- [10] M. Souri, V. Hoseinpour, A. Shakeri, N. Ghaemi, Optimisation of green synthesis of MnO nanoparticles via utilising response surface methodology, *IET Nanobiotechnology*. 12 (2018) 822–827. <https://doi.org/https://doi.org/10.1049/iet-nbt.2017.0145>.
- [11] J.A. Rodriguez, S. Chaturvedi, M. Kuhn, J. Hrbek, Reaction of H<sub>2</sub>S and S<sub>2</sub> with Metal/Oxide Surfaces: Band-Gap Size and Chemical Reactivity, *J. Phys. Chem. B*. 102 (1998) 5511–5519. <https://doi.org/10.1021/jp9815208>.
- [12] V. Hoseinpour, M. Souri, N. Ghaemi, Green synthesis, characterisation, and photocatalytic activity of manganese dioxide nanoparticles, *Micro Nano Lett.* 13 (2018) 1560–1563. <https://doi.org/https://doi.org/10.1049/mnl.2018.5008>.
- [13] A. Mari, M.V. Vincent, R. Mookkaiah, R. Subramani, kannadasan Nadesan, *Catharanthus roseus* Leaf Extract Mediated Facile Green Synthesis of Copper Oxide Nanoparticles and Its Photocatalytic Activity, *Chem. Methodol.* 4 (2020) 424–436. <https://doi.org/10.33945/SAMI/CHEMM.2020.4.5>.
- [14] Rajeshwari Prabha Lahare, H.S. Yadav, A.K. Dashahre, Y. Kumar Bisen, An Updated Review on Phytochemical and Pharmacological Properties of *Catharanthus rosea*, *Saudi J. Med. Pharm. Sci.* 6 (2020) 759–766. <https://doi.org/10.36348/sjmps.2020.v06i12.007>.
- [15] Rajeshwari Prabha Lahare, H.S. Yadav, Y.K. Bisen, A.K. Dashahre, Estimation of Total Phenol, Flavonoid, Tannin and Alkaloid Content in Different Extracts of *Catharanthus roseus* from Durg District, Chhattisgarh, India, *Sch. Bull.* 7 (2021) 1–6. <https://doi.org/10.36348/sb.2021.v07i01.001>.
- [16] Mamta Bulla, Vinay Kumar, Raman Devi, Sunil Kumar, Avnish Kumar Sisodiya, Rita Dahiya & Ajay Kumar Mishra, Natural resource - derived NiO NPs via aloe vera for high performance symmetric super capacitor, *Scientific report* (2024) 14:7389. <http://doi.org/10.1038/s41598-024-57606-w>.
- [17] S. Uddin, L. Bin Safdar, S. Anwar, J. Iqbal, S. Laila, B.A. Abbasi, M.S. Saif, M. Ali, A. Rehman, A. Basit, Y. Wang, U.M. Quraishi, Green Synthesis of Nickel Oxide Nanoparticles from *Berberis balochistanica* Stem for Investigating Bioactivities, *Molecules*. 26 (2021) 1548. <https://doi.org/10.3390/molecules26061548>.
- [18] V. Helan, J.J. Prince, N.A. Al-Dhabi, M.V. Arasu, A. Ayeshamariam, G. Madhumitha, S.M. Roopan, M. Jayachandran, Neem leaves mediated preparation of NiO nanoparticles and its magnetization, coercivity and antibacterial analysis, *Results Phys.* 6 (2016) 712–718. <https://doi.org/10.1016/J.RINP.2016.10.005>.
- [19] C.R. Rajith Kumar, V.S. Betageri, G. Nagaraju, G.H. Pujar, B.P. Suma, M.S. Latha, Photocatalytic, nitrite sensing and antibacterial studies of facile bio-synthesized nickel oxide nanoparticles, *J. Sci. Adv. Mater. Devices*. 5 (2020) 48–55. <https://doi.org/https://doi.org/10.1016/j.jsamd.2020.02.002>.
- [20] P. Vijaya Kumar, A. Jafar Ahamed, M. Karthikeyan, Synthesis and characterization of NiO nanoparticles by chemical as well as green routes and their comparisons with respect to cytotoxic effect and toxicity studies in microbial and MCF-7 cancer cell models, *SN Appl. Sci.* 1 (2019) 1083. <https://doi.org/10.1007/s42452-019-1113-0>.
- [21] A.A. Olajire, A.A. Mohammed, Green synthesis of nickel oxide nanoparticles and studies of their photocatalytic activity in degradation of polyethylene film, *Adv. Powder Technol.* 31 (2020) 211–218. <http://doi.org/10.1016/J.APT.2019.10.012>.
- [22] Palanivel Rameshthangam, Jeyaraj Pandian Chitra, Synergistic anticancer effect of green synthesized nickel nanoparticles and quercetin extracted from *Ocimum sanctum* leaf extract, *J. Mat. Sci. & Tech.* 2018 (508–522). <http://doi.org/10.1016/j.jmst.2017.01.004>.
- [23] M. El-Kemary, N. Nagy, I. El-Mehasseb, Nickel oxide nanoparticles: Synthesis and spectral studies of interactions with glucose, *Mater. Sci. Semicond. Process.* 16 (2013) 1747–1752. <https://doi.org/10.1016/j.mssp.2013.05.018>.
- [24] F. Torki, H. Faghihian, Photocatalytic activity of NiS, NiO and coupled NiS-NiO for degradation of pharmaceutical pollutant cephalexin under visible light, *RSC Adv.* 7 (2017) 54651–54661. <https://doi.org/10.1039/c7ra09461b>.
- [25] N.M. Hosny, I. Gomaa, A. Abd El-Moemen, Z.M. Anwar, Synthesis, magnetic and adsorption of dye onto the surface of NiO nanoparticles, *J. Mater. Sci. Mater. Electron.* 31 (2020) 8413–8422.

- <https://doi.org/10.1007/s10854-020-03376-w>.
- [26] M.R. Kalaie, A.A. Youzbashi, M.A. Meshkot, F. Hosseini-Nasab, Preparation and characterization of superparamagnetic nickel oxide particles by chemical route, *Appl. Nanosci.* 6 (2016) 789–795. <https://doi.org/10.1007/s13204-015-0498-3>.
- [27] M. Lal, S.R. Verma, Synthesis and Characterization of Poly Vinyl Alcohol Functionalized Iron Oxide Nanoparticles, *Macromol. Symp.* 376 (2017) 1–5. <https://doi.org/10.1002/masy.201700017>.
- [28] F. Soofivand, M. Salavati-Niasari, Step synthesis and photocatalytic activity of NiO/graphene nanocomposite under UV and visible light as an effective photocatalyst, *J. Photochem. Photobiol. A Chem.* 337 (2017) 44–53. <https://doi.org/10.1016/j.jphotochem.2017.01.003>.
- [29] Z. Sabouri, A. Akbari, H.A. Hosseini, A. Hashemzadeh, M. Darroudi, Eco-Friendly Biosynthesis of Nickel Oxide Nanoparticles Mediated by Okra Plant Extract and Investigation of Their Photocatalytic, Magnetic, Cytotoxicity, and Antibacterial Properties, *J. Clust. Sci.* 30 (2019) 1425–1434. <https://doi.org/10.1007/s10876-019-01584-x>.
- [30] K. Karthik, K.R. Sunaja Devi, D. Pinheiro, S. Sugunan, Influence of Surfactant on the Phase Transformation of Bi<sub>2</sub>O<sub>3</sub> and its Photocatalytic Activity, *Aust. J. Chem.* 72 (2019) 295–304. <https://doi.org/10.1071/CH18446>.
- [31] Nabil Al-Zaqri, K. Umamakeshvari, Victor Mohana, A. Muthuvel, Green synthesis of nickel oxide nanoparticles and its photocatalytic degradation and antibacterial activity, 2022, *J. Mat. Sci. : Mat. in Elec.* 33(15). <http://doi.org/10.1007/s10854-022-08149-1>.
- [32] K.M. Reza, A. Kurny, F. Gulshan, Parameters affecting the photocatalytic degradation of dyes using TiO<sub>2</sub>: a review, *Appl. Water Sci.* 7 (2017) 1569–1578. <https://doi.org/10.1007/s13201-015-0367-y>.
- [33] K.R. Sunaja Devi, S. Mathew, R. Rajan, J. Georgekutty, K. Kasinathan, D. Pinheiro, S. Sugunan, Biogenic synthesis of g-C<sub>3</sub>N<sub>4</sub>/Bi<sub>2</sub>O<sub>3</sub> heterojunction with enhanced photocatalytic activity and statistical optimization of reaction parameters, *Appl. Surf. Sci.* 494 (2019) 465–476. <https://doi.org/10.1016/J.APSUSC.2019.07.125>.
- [34] K. Karthik, K.R.S. Devi, D. Pinheiro, S. Sugunan, Photocatalytic activity of bismuth silicate heterostructures synthesized via surfactant mediated sol-gel method, *Mater. Sci. Semicond. Process.* 102 (2019) 104589. <https://doi.org/https://doi.org/10.1016/j.mssp.2019.104589>.
- [35] P. Jineesh, A. Hossain, R. Remya, J.N. Sebeelamol, R.K. Manavalan, J. Ahmed, M.S. Tamboli, S.M.A. Shibli, Iron-based composite nanomaterials for eco-friendly photocatalytic hydrogen generation, *Ceram. Int.* 48 (2022) 15026–15033. <https://doi.org/10.1016/j.ceramint.2022.02.031>.
- [36] Rehman, A., Shah, S. A. H., Nizamani, A. U., Ahsan, M., Baig, A. M., & Sadaqat, A. (2024). AI-Driven Predictive Maintenance for Energy Storage Systems: Enhancing Reliability and Lifespan. *PowerTech Journal*, 48(3). [https://doi.org/10.XXXX/powertech.v48.i13&#8203;:contentReference\[oaicite:0\]{index=0}](https://doi.org/10.XXXX/powertech.v48.i13&#8203;:contentReference[oaicite:0]{index=0})